H.W. KIM[✉]
N.H. KIM
C. LEE

An MOCVD route to In$_2$O$_3$ one-dimensional materials with novel morphologies

School of Materials Science and Engineering, Inha University, Incheon 402-751, Republic of Korea

ABSTRACT We have successfully synthesized one-dimensional (1-D) indium oxide (In$_2$O$_3$) arrays by the metalorganic chemical vapor deposition (MOCVD) method. We have characterized the products by means of X-ray diffraction (XRD), field-emission scanning electron microscopy (FE-SEM), and transmission electron microscopy (TEM). The SEM images showed that the 1-D materials with serrated surfaces had cross-sections in the shape of an acute triangle. The XRD and TEM studies revealed that the 1-D materials possessed a single-crystalline cubic structure and that the growth occurred preferentially along the [111] direction.

PACS 81.15.Gh

1   Introduction

One-dimensional (1-D) materials have attracted considerable attention because of their novel physical and chemical properties, which are different from those displayed by the same materials in the bulk state, and which give them the potential to be used for developing new types of devices [1, 2]. Since indium oxide (In$_2$O$_3$) is a transparent semiconducting oxide material, and, in particular, is an *n*-type semiconductor with a wide band gap, it has been extensively studied for many applications, such as photovoltaic devices, electro-optical devices, and sensors for oxidizing gases [3–8].

Up to the present, In$_2$O$_3$ 1-D materials including nanowires, nanobelts, nanofibers, and nanotubes have been mainly synthesized by the thermal heating or evaporation of In$_2$O$_3$ powders [9–12], In [13, 14], a mixture of In and In$_2$O$_3$ [15], and InP substrates [16]. In addition, various techniques, such as laser ablation [17], electrodeposition [18] sol–gel deposition [19], and nanocasting [20] have been successfully employed to make In$_2$O$_3$ 1-D materials.

Although the metalorganic CVD (MOCVD) method is supposed to be one of the simplest methods of the growing high-quality nanostructures, to the best of our knowledge, the production of In$_2$O$_3$ 1-D materials by the MOCVD technique has not previously been reported. In this paper, we investigate the possibility of growing single crystalline In$_2$O$_3$ 1-D

✉ Fax: +82-32-860-7544, E-mail: hwkim@inha.ac.kr

structures using a triethylindium (TEI) as a precursor in the presence of oxygen.

2   Experimental

The experiments were conducted in an MOCVD reactor and the schematic diagram of the reactor was previously reported [21]. A silicon (Si) (001) wafer (20 × 20 mm) was used as the deposition substrate. The substrate was cleaned in organic solvents and dried before loading it into the system.

High-purity Ar (99.999% purity) was passed through the TEI bubbler so as to deliver TEI vapor to the reactor. The TEI bubbler was maintained at a temperature of 35 °C. The In$_2$O$_3$ was synthesized by supplying O$_2$ and Ar gases, respectively, with flow rates of 5 and 20 standard cubic centimeters per minute (sccm). During the deposition process, the chamber pressure was maintained at 0.9 Torr. The heating process was continued for 60 minutes. Our previous experiments indicated that at the above process condition, the 1-D structure and the film-like structure were produced at substrate temperatures in the range of 350–375 °C and below 325 °C, respectively. The substrate temperature in this study was set to 350 °C.

The structural characterization of the products was performed by a Hitachi S-4200 field-emission scanning electron microscope (SEM), a Philips X'pert MPD X-ray diffractometer (XRD) with Cu K_α radiation, and a Philips CM-200 transmission electron microscope (TEM). The chemical compositions of the products were determined by an energy dispersive spectroscope (EDS) equipped in TEM. The TEM sample was prepared by stripping off and dispersing the substrate in acetone with the aid of ultrasonic vibration, and subsequently, by transferring a drop of solution onto a holey carbon film supported on a copper grid.

3   Results and discussion

Figure 1a shows the cross-sectional SEM image of the as-synthesized products. Close examination reveals that the products consist of a rod-like structure vertically aligned on the substrate. We observe that there is a film-like structure with a thickness of about 1–2 μm between the substrate and the rod-like structures. The average vertical growth rate is ∼ 14 μm/h. Figure 1b shows the plan-view SEM image, indicating that the products are almost uniformly distributed
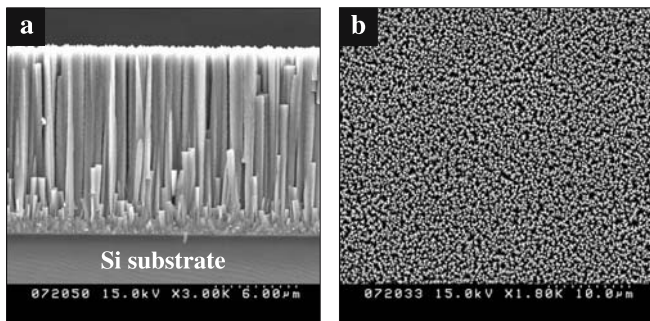
FIGURE 1 (**a**) Cross-sectional and (**b**) plan-view SEM images of the products
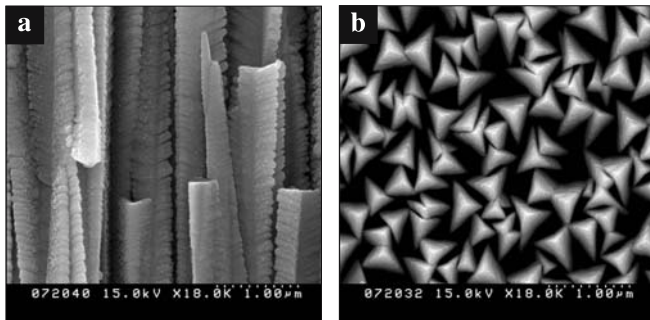
FIGURE 2 (**a**) Cross-sectional and (**b**) plan-view SEM images of the products from a closer view

FIGURE 3 XRD patterns of the products

over the entire substrate. Figure 2 shows the high magnification SEM images of the products. The cross sectional image (Fig. 2a) indicates that the products consist of 1-D materials with serrated surfaces. Although some of the 1-D materials were broken during the cross-sectional SEM sample preparation, we observe that the serrated surface of the stems of the 1-D material corresponds to arrays of "nanobumps". The plan-view SEM image (Fig. 2b) reveals that the 1-D materials have triangular cross sections with acute angles. From the top view, we reveal that the side length of the triangular cross section ranges from 200 to 700 nm.

Figure 3 shows the XRD pattern of the product. The θ–2θ scan data exhibit a main peak at 30.58° and a smaller peak at 63.67°, respectively, corresponding to the (222) and (444) diffraction peaks of the cubic bixbyite In_2O_3 phase (JCPDS 44-1087). Since the (222) and (444) diffraction peaks are significantly stronger than the neighboring diffraction peaks representing the other crystalline directions, which are invisible in this spectrum, we reveal that the product has a preferred orientation along the [111] direction. In addition, the θ–2θ scan data exhibit 2θ peaks at 69.13°, corresponding to the (004) peak of Si, which originates from the substrate.

The EDS analysis indicates that the 1-D materials consist of only In and O elements, regardless of position in the 1-D materials, from the stems to the ends. The typical EDS spectrum, recorded from a single 1-D material, is shown in Fig. 4a. The C- and Cu-related signals, are respectively, caused by contamination with C while preparing the TEM specimens and by the presence of Cu grids.

Figure 4b shows the side-view schematic drawing of a typical single 1-D material obtained in this study, with the length direction of the 1-D material and the nanobumps indexed.
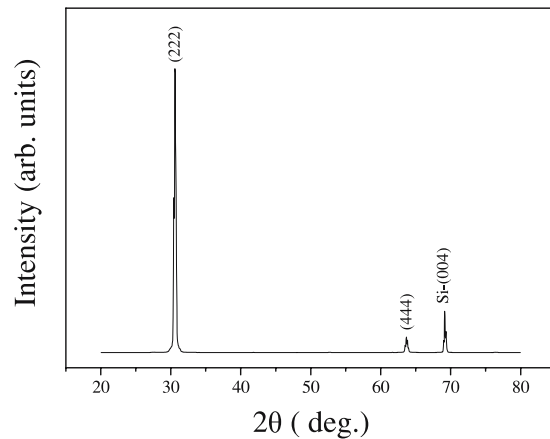
Figure 4c shows a TEM image of the tip of the 1-D material, indicating the rough surface. The 1-D material tapers gradually near the tip. No nanoparticles are found at the tip. Selected area electron diffraction (SAED) patterns, with the incident electron beam parallel to the [1$\bar{2}$1] direction, were recorded perpendicular to the long axis of the structure. The typical SAED pattern, which was found to be independent of the position in the 1-D structure, is shown in the inset. The reflections in the SAED pattern correspond to the lattice planes of bulk In_2O_3, indicating that the 1-D materials are single crystalline. Figure 4d shows the lattice resolved HRTEM image of the rectangular box marked in Fig. 4c. The interplanar spacings are approximately 0.29 nm and 0.72 nm, respectively, corresponding to the (222) and (10$\bar{1}$) planes of cubic In_2O_3. Figure 4e is a TEM image showing the nanobumps residing along the exterior of the 1-D material stem. The corresponding SAED pattern, recorded perpendicular to the nanobumps long axis, can be indexed for the [21$\bar{3}$] zone axis of crystalline In_2O_3. It is noteworthy that the length direction of the nanobump is along the [2$\bar{1}$1] direction and inclined at approximately 62° to the main axis direction of the 1-D materials. Figure 4f shows a lattice resolved HRTEM image representing the rectangular box marked in Fig. 4e. The interplanar spacings corresponding to the (222), (2$\bar{1}$1), and (031) planes of cubic In_2O_3 are approximately 0.29 nm, 0.41 nm, and 0.32 nm, respectively, revealing that the nanobumps are single crystalline.

Since the SEM images, TEM images and EDS measurement coincidentally indicate that all of the structure tips are free of metal nanoparticles, we surmise that the growth of the In_2O_3 structures in the present route is not dominated by a tip-growth vapor–liquid–solid mechanism. The 1-D material arrays may not grow directly from the Si substrate, but from the layer of In_2O_3 predeposited on top of the Si substrate (Fig. 1a). Our preliminary experiments confirmed that an approximately 1 μm-thick film without the 1-D material was fabricated with a deposition time of 5 minutes, and that the 1-D materials started to appear on the film-like structure after a deposition time of 10 minutes (not shown here). The transition from two- to three-dimensional growth may occur in the initial stages of the deposition process. We suppose that, in the present case, the synthesis of 1-D materials consists of several growth phases, such as nucleation, thin film
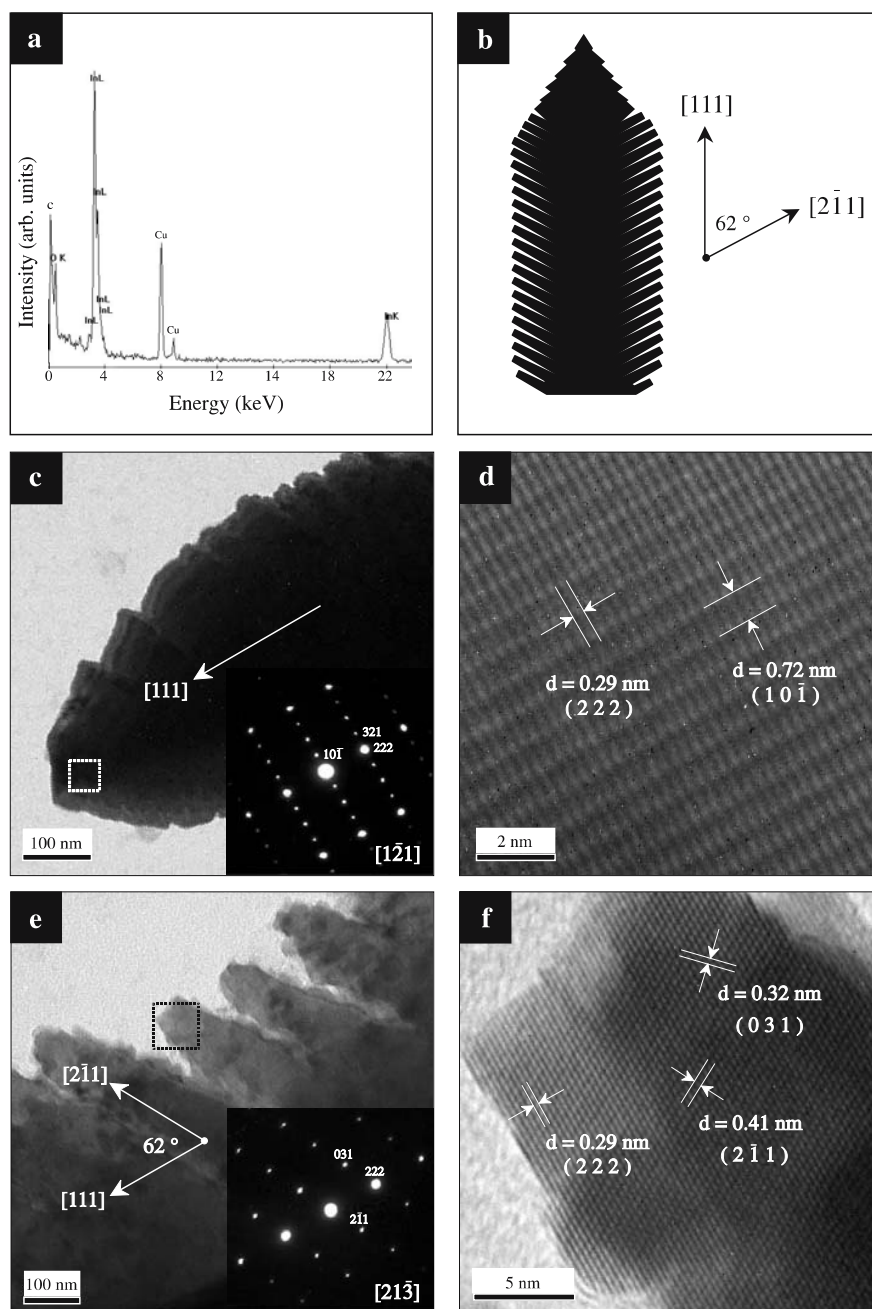
FIGURE 4 (**a**) Typical EDS spectrum and (**b**) side-view schematic drawing of a single 1-D material. (**c**) TEM image showing the tip part of an individual 1-D material. The *inset* shows a typical SAED pattern taken perpendicular to the stem of the 1-D materials. (**d**) Lattice-resolved HRTEM image of the rectangular box marked in Fig. 4c. (**e**) TEM image showing nanobumps residing along the exterior of an individual 1-D material. The *inset* is a SAED pattern taken perpendicular to the stem of the nanobumps. (**f**) Lattice-resolved HRTEM image corresponding to the rectangular box marked in Fig. 4e

formation, rod-like structure elongation and nanobump formation. However, when the rod-like structures reach a certain height, the underlayer thickening process ceases, due mostly likely to the limited mass transfer of the In and O species. An intensive investigation is required to determine the exact mechanism for the formation of In$_2$O$_3$ 1-D materials in the present work.

Up to the present, several researchers have reported the preparation of the In$_2$O$_3$ 1-D structures with conventional morphologies such as the nanotubes with a hollow cavity [15, 19], the nanobelts or nanofibers which have rectangular cross-sections with different width-to-thickness ratios [9, 14, 16], and the solid nanowires with a circular cross-section [10, 11, 13, 17, 18, 20]. Nguyen et al. reported the preparation of the aligned 1-D structures with novel mor-

phologies, consisting of square columnar vertical bodies [12]. On the other hand, the 1-D structures produced in the present work consist of columnar vertical bodies with an acute-angled triangular cross-section. Therefore, to the best of our knowledge, this is the first report on the production of the aligned 1-D In$_2$O$_3$ structures with a triangular cross-section.

4   Conclusion

In summary, we demonstrated the production of dense arrays of well aligned In$_2$O$_3$ 1-D materials using an MOCVD method. These 1-D materials are vertically aligned on the substrate. Each individual 1-D material has a cross section in the shape of an acute triangle with a typical side length of less than 1 μm, and has a serrated surface, consisting of

single crystalline nanobumps. These 1-D materials consist of single-crystal cubic structures with their axis directions in the [111] direction.

REFERENCES

1 C.R. Martin: Science **266**, 1961 (1994)
2 W. Schwarzacher, O.I. Kasyutich, P.R. Evans, M.G. Darbyshire, G. Yi, V.M. Fedosyuk, F. Rousseaux, E. Cambril, D. Decanini: J. Magn. Magn. Mater. **198–199**, 185 (1999)
3 K. Hara, T. Horiguchi, T. Kinoshita, K. Sayama, H. Sogihara, H. Arakawa: Solar Energy Mater. Solar Cells **64**, 115 (2000)
4 K.L. Chopra, S. Major, D.K. Pandya: Thin Solid Films **102**, 1 (1983)
5 H. Kominami, T. Nakamura, K. Sowa, Y. Nakanishi, Y. Hatanaka, G. Shimaoka: Appl. Surf. Sci. **113–114**, 519 (1997)
6 H. Yamaura, T. Jinkawa, J. Tamaki, K. Moriga, N. Miura, N. Yamazoe: Sensor. Actuator B **35–36**, 325 (1996)
7 A. Gurlo, N. Barsan, M. Ivanovskaya, U. Weimer, W. Gopel: Sens. Actuators, B **47**, 92 (1998)
8 M.Z. Atashbar, B. Gong, H.T. Sun, W. Wlodarski, R. Lamb: Thin Solid Films **354**, 222 (1999)
9 Z.W. Pan, Z.R. Dai, Z.L. Wang: Science **291**, 1947 (2001)
10 J. Zhang, X. Qing, F.H. Jiang, Z.H. Dai: Chem. Phys. Lett. **371**, 311 (2003)
11 X.C. Wu, J.M. Hong, Z.J. Han, Y.R. Tao: Chem. Phys. Lett. **373**, 28 (2003)
12 P. Nguyen, H.T. Ng, T. Yamada, M.K. Smith, J. Li, J. Han, M. Meyyappan: Nano Lett. **4**, 651 (2004)
13 X.S. Peng, G.W. Meng, J. Zhang, X.F. Wang, Y.W. Wang, C.Z. Wang, L.D. Zhang: J. Mater. Chem. **12**, 1602 (2002)
14 J.S. Jeong, J.Y. Lee, C.J. Lee, S.J. An, G.C. Yi: Chem. Phys. Lett. **384**, 246 (2004)
15 Y. Li, Y. Bando, D. Golberg: Adv. Mater. **15**, 581 (2003)
16 C.H. Liang, G.W. Meng, Y. Lei, F. Phillipp, L.D. Zhang: Adv. Mater. **13**, 1330 (2001)
17 C. Li, D.H. Zhang, S. Han, X.L. Liu, T. Tang, C.W. Zhou: Adv. Mater. **15**, 143 (2003)
18 M.J. Zheng, L.D. Zhang, G.H. Li, X.Y. Zhang, X.F. Wang: Appl. Phys. Lett. **79**, 839 (2001)
19 B. Cheng, E.T. Samulski: J. Mater. Chem. **11**, 2901 (2001)
20 H.F. Yang, Q.H. Shi, B.Z. Tian, Q.Y. Lu, F. Gao, S.H. Xie, J. Fan, C.Z. Yu, B. Tu, D.Y. Zhao: J. Am. Chem. Soc. **125**, 4724 (2003)
21 H.W. Kim, N.H. Kim: Appl. Surf. Sci. **230**, 301 (2004)